Aptamers evolved from live cells as effective molecular probes for cancer study

Dihua Shangguan*, Ying Li†, Zhiwen Tang*, Zehui Charles Cao*, Hui William Chen*, Prabodhika Mallikaratchy*, Kwame Sefah*, Chaoyong James Yang*, and Weihong Tan*‡

*Center for Research at the Bio/Nano Interface, Department of Chemistry, Shands Cancer Center, University of Florida Genetics Institute and McKnight Brain Institute, and †Department of Pathology, Shands Cancer Center, Shands Hospital, College of Medicine, University of Florida, Gainesville, FL 32611-7200

Edited by Mark A. Ratner, Northwestern University, Evanston, IL, and approved June 13, 2006 (received for review March 31, 2006)

Using cell-based aptamer selection, we have developed a strategy to use the differences at the molecular level between any two types of cells for the identification of molecular signatures on the surface of targeted cells. A group of aptamers have been generated for the specific recognition of leukemia cells. The selected aptamers can bind to target cells with an equilibrium dissociation constant (K_d) in the nanomolar-to-picomolar range. The cell-based selection process is simple, fast, straightforward, and reproducible, and, most importantly, can be done without prior knowledge of target molecules. The selected aptamers can specifically recognize target leukemia cells mixed with normal human bone marrow aspirates and can also identify cancer cells closely related to the target cell line in real clinical specimens. The cell-based aptamer selection holds a great promise in developing specific molecular probes for cancer diagnosis and cancer biomarker discovery.

cell-based selection | cell imaging | DNA aptamers

Understanding of human diseases at the molecular level has been extremely challenging because of the lack of effective probes to identify and recognize distinct molecular features of diseases. Cancers, as well as many other diseases, are originated from the mutations of human genes. Such genetic alterations result in not only different behaviors of the diseased cells, but also changes of the cells at the morphological and molecular levels. Traditionally, cancers are diagnosed mostly based on the morphology of tumor tissues or cells. However, these morphologic features are difficult to be used to carry out early cancer diagnosis or to evaluate the complex molecular alterations that lead to cancer progression (1, 2). Therefore, molecular characteristics, especially at the proteomic level, should be used to classify cancers because of the direct connection between genetic features and protein expression. Cancer diagnosis based on molecular features can be highly specific and extremely sensitive when incorporated with proper signal transduction and amplification mechanisms. Nonetheless, identification of molecular signatures of a particular cancer remains a great challenge, if not impossible, which is reflected by the fact that very few biomarkers are available for effective cancer diagnosis.

Molecular-level differences are present between any two given types of cells, such as normal vs. tumor cells and tumor cell type 1 vs. type 2. These differences possess great significance in aiding the understanding of the biological processes and mechanisms of diseases. They could also be highly useful for disease diagnosis, prevention, and therapy. However, identifying molecular differences between any two types of cells is not an easy task with current technologies. For example, discovery of unknown molecular features of diseased cells by using molecular probes is almost impractical because most of today's methodologies rely on known biomarkers for the development of corresponding molecular probes, which has been proved insufficient for addressing many emerging medical problems. Even if the molecular-level differences can be identified, there is still a need to validate that the specific differences are indeed meaningful and vital for the desired biomedical property or the disease before any real clinical applications can be benefited.

Despite all of the difficulties, a practical strategy that could compare cancer cells with normal cells and identify the differences at the molecular level is highly desirable to facilitating the discovery of molecular features of cancer cells. Here, we report a systematic approach that can conveniently circumvent the limitations of current technologies. A new class of molecular probes termed aptamers have been isolated and identified for the recognition of molecular differences expressed on the surface membranes of two different types of cells. These probes can be used to specifically detect target cancer cells based on molecular characteristics in the presence of other cells, leading to effective disease studies and early diagnosis.

Aptamers are ssDNA, RNA, or modified nucleic acids. They have the ability to bind specifically to their targets, which range from small organic molecules to proteins (3–5). The basis for target recognition is the tertiary structures formed by the single-stranded oligonucleotides (6). Aptamers are obtained through an *in vitro* selection process known as SELEX (systematic evolution of ligands by exponential enrichment) (7, 8), in which aptamers are selected from a library of random sequences of synthetic DNA or RNA by repetitive binding of the oligonucleotides to target molecules. Aptamers have had many important applications in bioanalysis, biomedicine, and biotechnology (9–12). Most aptamers reported so far have been selected by using simple targets, such as a purified protein. Recently, aptamer selection against complex targets, such as red blood cell membranes and endothelial cells, was also demonstrated (13–16). Compared with molecular probes currently available for biomarker recognition, aptamers are emerging candidates with ample potential due to their high specificity, low molecular weight, easy and reproducible production, versatility in application, and easy discovery and manipulation (17). Currently, the application of aptamers toward medical research and application is limited because of the lack of aptamers for systems of medical relevance. Thus, the major goal in this study is the development and utilization of a group of effective aptamers for leukemia studies.

To identify unique molecular features of target cancer cells, we have developed a cell-based SELEX (cell-SELEX) for the selection of a panel of target cell-specific aptamers. A counter-selection strategy is used to collect DNA sequences that only interact with the target cells but not the control cells. Consequently, aptamer candidates exclusively binding to the target cells are enriched. The membrane protein targets of the selected aptamers represent the molecular-level differences between the two cell lines used in this study. Not only can molecular signatures of the cancer cells be easily discovered, but probes that can recognize such unique features with very high affinity and specificity are also generated at the same time. More impor-

Conflict of interest statement: No conflicts declared.

This paper was submitted directly (Track II) to the PNAS office.

Abbreviations: ALL, acute lymphoblastic leukemia; SELEX, systematic evolution of ligands by exponential enrichment; TAMRA, tetramethylrhodamine anhydride.

‡To whom correspondence should be addressed. E-mail: tan@chem.ufl.edu.

www.pnas.org/cgi/doi/10.1073/pnas.0602615103

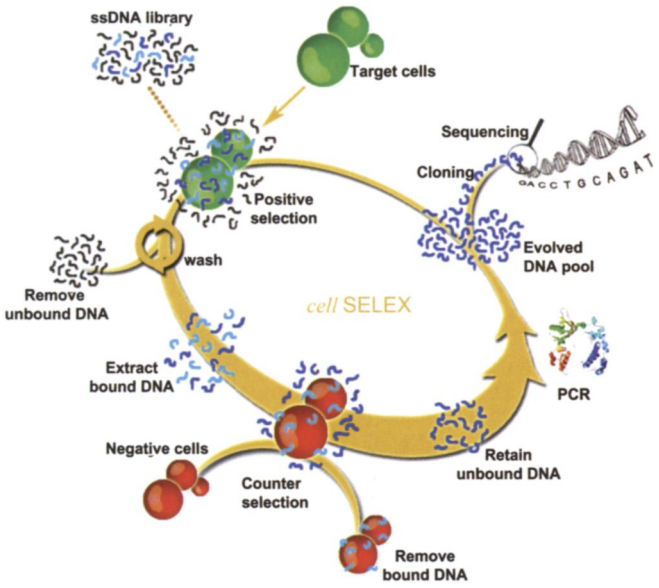

Fig. 1. Schematic representation of the cell-based aptamer selection. Briefly, the ssDNA pool was incubated with CCRF-CEM cells (target cells). After washing, the bound DNAs were eluted by heating to 95°C. The eluted DNAs were then incubated with Ramos cells (negative cells) for counterselection. After centrifugation, the supernatant was collected and the selected DNA was amplified by PCR. The PCR products were separated into ssDNA for next-round selection or cloned and sequenced for aptamer identification in the last-round selection.

tantly, the use of a panel of probes has the clear advantage over the single-biomarker-based assays in clinical practice, providing much more information for accurate disease diagnosis and prognosis. At the same time, the probes recognize the targets at their native state, creating a true molecular profile of the disease cells. This is important in clinical application of the molecular probes. In addition, the aptamers selected from cell-SELEX offer valuable tools for isolating and identifying new biomarkers of the diseased cells if desired. The development of specific probes for molecular signatures on the cancer cell surface will provide new opportunities in "personalized" medicine.

Results and Discussion

Cell-SELEX for Enrichment of Aptamer Candidates for Target Cells. The process of our cell-SELEX is illustrated in Fig. 1, and the detailed procedures are provided in *Experimental Procedures*. Two hematopoietic tumor cell lines were chosen as a model system for our aptamer selection because they are well studied and consist of relatively homogeneous tumor cells. In addition, flow cytometry analysis can be easily carried out to monitor the selection process and to evaluate the selected aptamers for their capability of recognizing target cells. A cultured precursor T cell acute lymphoblastic leukemia (ALL) cell line, CCRF-CEM, was used as the target for aptamer selection. A B cell line from human Burkitt's lymphoma, Ramos, was used as the negative control to reduce the collection of DNA sequences that could bind to common surface molecules present on both types of cells.

In our selection, a library of ssDNAs that contained a 52-mer random sequence region flanked by two 18-mer PCR primer sequences was used. The library was incubated with the target cells to allow binding to take place. The cells were then washed, and the DNA sequences bound to the cell surface were eluted. The collected sequences were then allowed to interact with excess negative control cells, and only the DNA sequences remaining free in the supernatant were collected and amplified for the next-round selection. After multiround selection, the subtraction process efficiently reduced the DNA sequences that bound to the control cells, while those target-cell-specific aptamer candidates were enriched.

The progress of the selection process was monitored by using flow cytometry. DNA products collected after each round were labeled with FITC dye and incubated with live cells. The fluorescence intensity of the labeled cells measured by the flow cytometry analysis represented the binding capacity of the enriched DNA pool to the cells. With the increasing number of selection cycles, steady increases in fluorescence intensity on the CCRF-CEM cells (target cells) were observed (Fig. 2*A*), indicating that DNA sequences with better binding affinity to the target cells were enriched. Nevertheless, there was no significant change in fluorescence intensity on the Ramos cells (control cells). These results indicate that the DNA probes specifically recognizing unique surface targets on CCRF-CEM cells were isolated. The specific binding of the selected pools to the target cells was further confirmed by confocal imaging (Fig. 2*B*). After incubation with a tetramethylrhodamine anhydride (TAMRA) dye-labeled aptamer pool, the CEM cells presented very bright fluorescence on their periphery, whereas the Ramos cells displayed weak fluorescence.

Identification of Aptamers for the Target Cells. It usually took ≈20 rounds to achieve excellent enrichment of aptamer candidates.

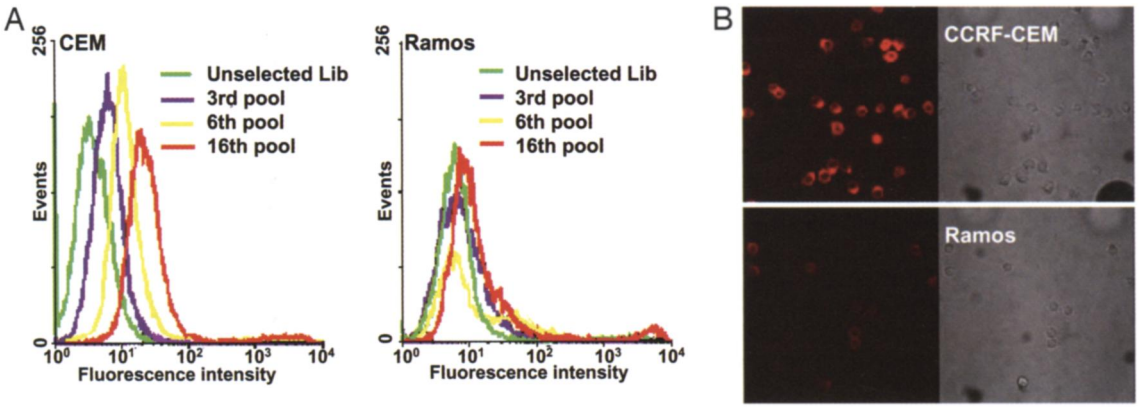

Fig. 2. Binding assay of selected pool with CCRF-CEM and Ramos cells. (*A*) Flow cytometry assay to monitor the binding of selected pool with CCRF-CEM cells (target cells) and Ramos cells (negative cells). The green curve represents the background binding of unselected DNA library. For CEM cells, there was an increase in binding capacity of the pool as the selection was progressing, whereas there was little change for the control Ramos cells. (*B*) Confocal imaging of cells stained by the 20th-round selected pool labeled with tetramethylrhodamine dye molecules. (*Upper Left*) Fluorescence image of CCRF-CEM cells. (*Upper Right*) Optical image of CCRF-CEM cells. (*Lower Left*) Fluorescence image of Ramos cells. (*Lower Right*) Optical image of Ramos cells.

Table 1. Binding affinity of the selected aptamer sequences

Sequence name	K_d, nM
sgc3	1.97 ± 0.29
sgc6	8.76 ± 0.62
sgd3	3.58 ± 0.58
sgc4	26.6 ± 2.1
sgc4a	229 ± 38
sgc5	113 ± 41
sgc7	144 ± 75
sgc8	0.80 ± 0.09
sga16	5.00 ± 0.52
Sgd2	7.21 ± 0.89

The highly enriched aptamer pools were cloned and sequenced by using a high-throughput genome sequencing method. The sequences were grouped based on the homology of the DNA sequences of individual clones with each group containing very similar sequences.

Twenty sequences were chosen for further characterization because they were highly abundant in their family. The binding assays of the selected sequences with target cells were performed by using flow cytometry. Thirteen sequences revealed obvious binding to CCRF-CEM cells. Moreover, the binding was not interfered with by the addition of 1,000-fold excess of starting DNA library. Except aptamers such as sgd2, sgc4, and its homologue sgc4a, which could recognize both CCRF-CEM and Ramos cells (data not shown), other aptamers only recognized the target cell line, CCRF-CEM. Ten aptamers were confirmed to have high affinity for CCRF-CEM cells with calculated equilibrium dissociation constants (K_d) in the nanomolar-to-picomolar range, and their K_d are listed in Table 1. CD2, CD3, CD4, CD5, CD7, and CD45 are the surface antigens expressed on CCRF-CEM cells, and none of our tested aptamer sequences showed any evidence of competition with antibodies against these antigens (data not shown). This finding indicates that the aptamers may interact with unique surface-binding entities.

Cell-SELEX Generates High-Affinity Molecular Probes for Target Cells. We tested the individual aptamers. As shown in Fig. 3 *A* and *B*, aptamers sga16 (K_d = 5.00 ± 0.52 nM) and its homologues sgc8 (K_d = 0.80 ± 0.09 nM) can specifically recognize the CCRF-CEM cells with high affinity. The specificity of both aptamers was also observed directly by using confocal imaging. Intense fluorescence from sga16 bound on the CCRF-CEM cell surface was observed, whereas the Ramos cells had no obvious fluorescence. These results clearly demonstrate the great potential of using aptamers sga16 and sgc8 as excellent molecular probes for CCRF-CEM-cell recognition.

It is worth noting that some of our selected aptamers can identify binding entities expressed only by a small subset of target cells. Sequences sgc3 (K_d = 1.97 ± 0.29 nM), sgc6 (K_d = 8.76 ± 0.62 nM), and sgd3 (K_d = 3.58 ± 0.58 nM) were found to bind only to a small population of the CCRF-CEM cells (≈20–40% of the cells) (the second peak in Fig. 4*A* and the yellow area in Fig. 4*C*) with high affinity, but they did not bind to Ramos cells. Sgc3 and sgc6 are, in fact, homologues, whereas sequence sgd3 is very different from them. Confocal imaging also confirmed that aptamer sgc3 strongly bound to a subset of CCRF-CEM cells (Fig. 4*B*). These sgc3-labeled cells showed the same forward- and side-scatter properties as the rest of the sgc3-negative cells in flow cytometry assays, indicating that they were viable cells. We have also immunophenotyped the sgc3-labeled cells and confirmed that they were CD5- and CD7-positive neoplastic T cells rather than contaminations from other types of cells (Fig. 4*C*). On the other hand, the sgc3-binding CCRF-CEM cells were CD3-negative, implying that they might represent a unique differentiation stage or phase of the cell cycles.

The reason behind our observations might be that a subpopulation of the target cells had unique molecular signatures expressed on the cell surface. It is interesting but not surprising to see that the cell-based SELEX could generate molecular probes specific for only a fraction of the target cells. Considering the principles of cell-SELEX, any molecular differences between the target and control cells could lead to the selection of aptamers that can recognize such differences, no matter whether they are present on all or just part of the target cells.

The Selected Aptamers Can Be Used for Highly Specific Recognition of Target Cells in Real Biological Samples. To test the feasibility of the selected aptamers as probes for specific molecular recognition, FITC-labeled aptamers (sgc8, sgc3, sgd3, sgc4, and sgd2) and monoclonal antibodies were used to detect CCRF-CEM leukemia cells mixed with normal human bone marrow aspirates. The human bone marrow aspirates consisted of mature and immature granulocytes, nucleated erythrocytes, monocytes, mature and immature B cells, and T cells. As expected, sgc8, sgc3, and sgd3 only recognized cultured leukemia T cells (CCRF-CEM) (Fig. 5) and did not bind to normal CD3-positive T cells or any other bone marrow cells. Aptamers sgc4 and sgd2 slightly bound to mature and immature B cells, a subset of CD3-positive T cells, nucleated erythrocytes from the human bone marrow, and cultured leukemia T cells (CCRF-CEM) (data not shown).

Aptamers (sgc8, sgc3, sgd3, sgc4, and sgd2) were all found to recognize other T cell ALL cell lines, Sup-T1, Molt-4, and Jurkat, but not all could bind to cultured B cells and AML cells (Table 2). Recognition of tumor cells in real clinical samples by our aptamers was also tested. Patients' bone marrow aspirates were examined with FITC-labeled aptamers and monoclonal antibodies. The re-

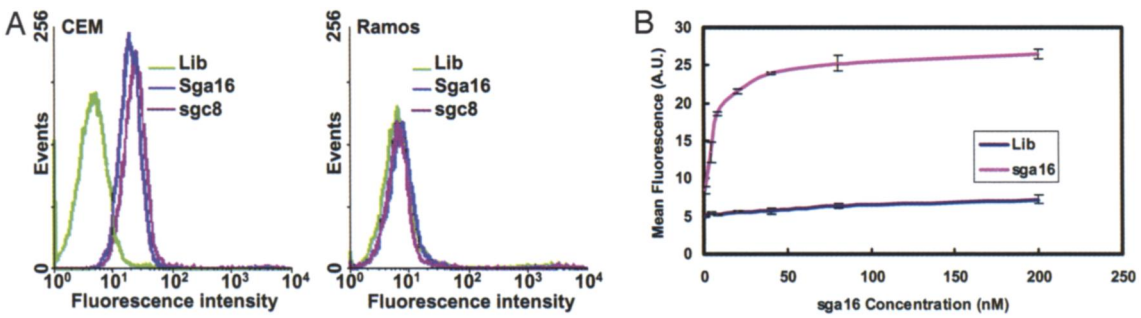

Fig. 3. Characterization of selected aptamers. (*A*) Flow cytometry assay for the binding of the FITC-labeled sequences sga16 and sgc8 with CCRF-CEM cells (target cells) and Ramos cells (negative cells). The green curve represents the background binding of unselected DNA library. The concentration of the aptamers in the binding buffer was 250 nM. (*B*) Flow cytometry to determine the binding affinity of the FITC-labeled aptamer sequence sga16 to CCRF-CEM cells. The nonspecific binding was measured by using FITC-labeled unselected library DNA.

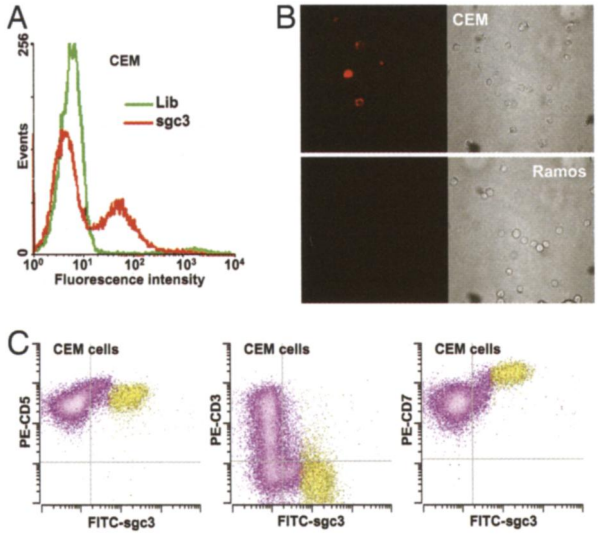

Fig. 4. Aptamer sgc3 only recognizes a subset of CCRF-CEM cells. (*A*) Flow cytometry assay for the binding of the FITC-labeled sequence sgc3 with CCRF-CEM cells (target cells). The green curve represents the background binding of unselected DNA library. The second peak of the red curve represents the sgc3-labeled subset of cells. The concentration of the aptamer in the binding buffer was 250 nM. (*B*) Fluorescence confocal images of CEM and Ramos cells stained by sgc3 labeled with TAMRA. (*Left*) Fluorescence images of CCRF-CEM cells and Ramos cells. (*Right*) Optical images of CCRF-CEM cells and Ramos cells. (*C*) Flow cytometry assay for the binding of CCRF-CEM cells to aptamer sgc3 and monoclonal antibodies against CD5, CD7, and CD3. The yellow area represents the sgc3-labeled subset of cells. Aptamer sgc3 selectively bound to a subpopulation of CCRF-CEM cells, which expressed abundant CD7 and CD5 but not CD3. The final concentration of sgc3 in the binding buffer was 250 nM.

sults (Table 2) revealed that none of aptamers (sgc8, sgc3, sgd3, sgc4, and sgd2) could recognize the cancer cells from B cell lymphoma patients but all were able to bind the cancer cells from T cell ALL patients (Fig. 6), which were closely related to the CCRF-CEM target cells used in our cell-SELEX. The capability of the aptamers selected in our cell-SELEX for molecular diagnosis in clinical practice is clearly demonstrated here.

The Binding Sites of the Aptamers on the Target Cells. To test preliminarily whether the targets of the aptamers are membrane proteins on the cell surface, we treated CCRF-CEM cells with proteinases such as trypsin and proteinase K for a short time before adding the aptamer to these treated cells. As shown in Fig. 7, after treating the cells with trypsin or proteinase K for 10 min, aptamer sgc8, sgc3, and sgd3 lost their binding to these cells, whereas the interactions of aptamer sgd2 and sgd4 with the cells were not affected. It can be deduced that the binding entities of aptamer sgc8, sgc3, and sgd3 had been removed by the proteinases, indicating that the target molecules were most likely membrane proteins. Interestingly, the targets of aptamers sgd2 and sgc4 were clearly not affected by the proteinases.

In conclusion, a cell-based SELEX strategy has been developed to generate a panel of aptamers as useful molecular probes to reveal the molecular-level differences between any two types of cells. The selected aptamers have then been used for the specific recognition of diseased cells. Molecular differences between the target and control cells could be isolated easily, providing an effective approach to the discovery of molecular signatures of many other diseases. More importantly, detailed knowledge of the distinct targets on the cell surface is not needed before the selection, which could greatly simplify the process of molecular probe development. The entire selection process is simple, fast, reproducible, and straightforward, and the selected

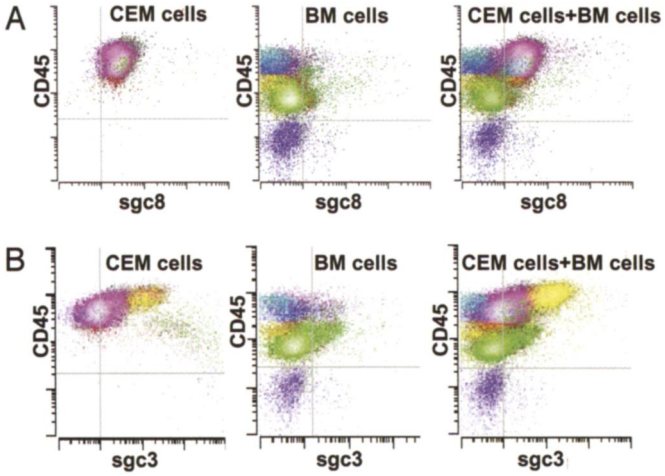

Fig. 5. Molecular recognition of CCRF-CEM cells and human bone marrow cells incubated with FITC-labeled sgc8, sgc3, and peridinin chlorophyll protein-labeled anti-CD45 antibody. The aptamer sgc8 or sgc3 and monoclonal antibodies were incubated with the target CCRF-CEM cells and/or bone marrow cells. The sgc8 (*A*) and sgc3 (*B*) were able to recognize the target leukemia cells selectively when CCRF-CEM leukemia cells were mixed with cells from human bone marrow aspirates.

aptamers can specifically bind to target cells with K_d in the nanomolar-to-picomolar range. Some of the aptamers can recognize a small subset of the target cells. Target cells mixed with normal human bone marrow aspirate can be readily distinguished. In addition, cancer cells from clinical patients' specimens, which are closely related to the target cells, were also recognized by the selected aptamers. Furthermore, the aptamers can be used to isolate the disease-specific protein targets to facilitate the discovery of clinically important biomarkers. Our preliminary results have suggested that the binding sites of the selected aptamers are most likely proteins on cell-membrane surfaces. The development of specific probes for molecular signatures on the cancer cell surface will allow us to define tumors, create tailored treatment regime for more "personal-

Table 2. Using aptamers to recognize cancer cells

Cell line	sgc8	sgc3	sgc4	sgd2	sgd3
Cultured cell lines					
Molt-4 (T cell ALL)	++++	+++	++++	++++	++++
Sup-T1 (T cell ALL)	++++	+	++++	++++	++
Jurkat (T cell ALL)	++++	+++	++++	++++	++++
SUP-B15 (B cell ALL)	+	0	++	+	0
U266 (B cell myeloma)	0	0	0	0	0
Toledo (B cell lymphoma)	0	0	++++	++++	+
Mo2058 (B cell lymphoma)	0	++	++	0	+
NB-4 (AML, APL)	0	0	+++	++++	0
Cells from patients					
T cell ALL	++	+++	+++	+++	+++
Large B cell lymphoma	0	0	0	0	0

A threshold based on fluorescence intensity of FITC in the flow-cytometric analysis was chosen so that 99% of cells incubated with the FITC-labeled unselected DNA library would have fluorescence intensity below it. When the FITC-labeled aptamer was allowed to interact with the cells, the percentage of the cells with fluorescence above the set threshold was used to evaluate the binding capacity of the aptamer to the cells. 0, <10%; +, 10–35%; ++, 35–60%; +++, 60–85%; ++++, >85%; AML, acute myeloid leukemia; APL, acute promyelocytic leukemia.

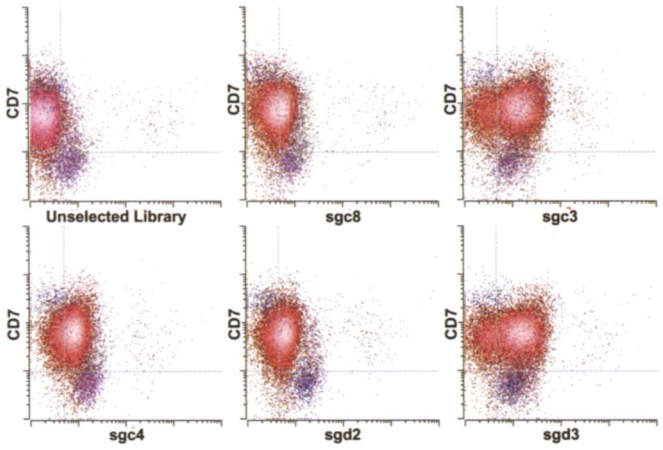

Fig. 6. Molecular recognition of T-ALL cells in patient bone marrow aspirates with FITC-labeled sgc8, sgc3, sgc4, sgd2, sgd3, and R-phycoerythrin-labeled anti-CD7 antibody. The background was measured by using FITC-labeled unselected library. The red dots represent T-ALL cells.

ized" medicine, monitor the response to therapy, and detect minimal residual diseases.

Experimental Procedures

Cell Lines and Buffers. CCRF-CEM (CCL-119, T cell line, human ALL), Ramos (CRL-1596, B cell line, human Burkitt's lymphoma), Toledo (CRL-2631, B cell line, human diffuse large-cell lymphoma), Sup-T1 (CRL-1942, T cell line, human lymphoblastic leukemia), Jurkat (TIB-152, human acute T cell leukemia), Molt-4 (CRL-1582, T cell line, human ALL), SUP-B15 (CRL-1929, B lymphoblast, human ALL), and U266 (TIB-196, B lymphocyte, human myeloma, plasmacytoma) were obtained from American Type Culture Collection. Mo2058 (Mantle-cell lymphoma, Epstein–Barr virus-positive cell line) and NB-4 (acute promyelocytic leukemia) were obtained from the Department of Pathology at the University of Florida. All of the cells were cultured in RPMI medium 1640 (American Type Culture Collection) supplemented with 10% FBS (heat-inactivated; GIBCO) and 100 units/ml penicillin–streptomycin (Cellgro). Cells were washed before and after incubation with wash buffer [4.5 g/liter glucose and 5 mM $MgCl_2$ in Dulbecco's PBS with calcium chloride and magnesium chloride (Sigma)]. Binding buffer used for selection was prepared by adding yeast tRNA (0.1 mg/ml; Sigma) and BSA (1 mg/ml; Fisher) into wash buffer to reduce background binding. Antibodies against CD2, CD3, CD4, CD5, CD7, and CD45 were purchased from BD Biosciences. Trypsin and proteinase K were purchased from Fisher Biotech.

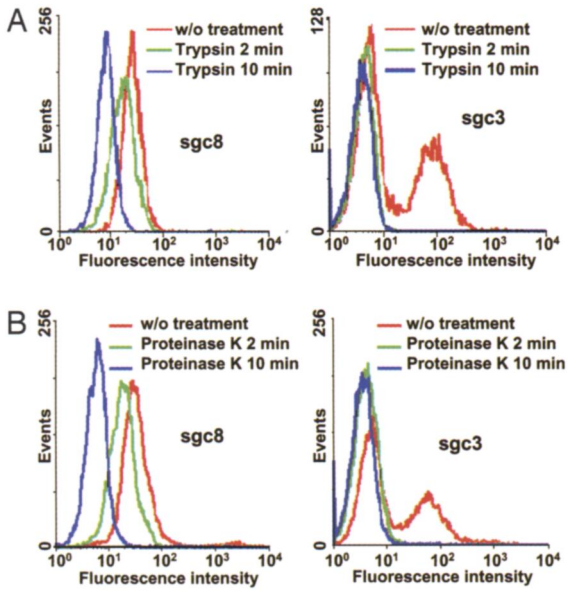

Fig. 7. Binding of aptamers sgc8 and sgc3 to trypsin-treated (*A*) or proteinase K-treated (*B*) CCRF-CEM cells. The concentration of the aptamers in the binding buffer was 250 nM.

SELEX Library and Primers. The HPLC-purified library contained a central randomized sequence of 52 nucleotides flanked by two 18-nt primer hybridization sites (5′-ATA CCA GCT TAT TCA ATT- 52-nt -AGA TAG TAA GTG CAA TCT-3′). An FITC-labeled 5′ primer (5′-FITC-ATA CCA GCT TAT TCA ATT-3′) or a TAMRA-labeled 5′ primer (5′-TAMRA-ATA CCA GCT TAT TCA ATT-3′), and a triple-biotinylated (trB) 3′ primer (5′-trB-AGA TTG CAC TTA CTA TCT-3′) were used in the PCRs for the synthesis of double-labeled, double-stranded DNA molecules. After denaturing in alkaline condition (0.2 M NaOH), the FITC-conjugated sense ssDNA strand was separated from the biotinylated antisense ssDNA strand with streptavidin-coated Sepharose beads (Amersham Pharmacia Biosciences) and used for next-round selection. The selection process was monitored by using flow cytometry.

SELEX Procedures. The procedures of selection were as follows. The ssDNA pool (200 pmol) dissolved in 400 μl of binding buffer was denatured by heating at 95°C for 5 min and cooled on ice for 10 min before binding. Then the ssDNA pool was incubated with 1–2 $\times$ 10^6 CCRF-CEM cells (target cells) on ice for 1 h. After washing, the bound DNAs were eluted by heating at 95°C for 5 min in 300 μl of binding buffer. The eluted DNAs were then incubated with Ramos cells (negative cells; 5-fold excess than CCRF-CEM cells) on ice for counterselection for 1 h. After centrifugation, the supernatant was desalted and then amplified by PCR with FITC- or biotin-labeled primers (10–20 cycles of 0.5 min at 94°C, 0.5 min at 46°C, and 0.5 min at 72°C, followed by 5 min at 72°C; the *Taq* polymerase and dNTPs were obtained from Takara). The selected sense ssDNA was separated from the biotinylated antisense ssDNA strand by streptavidin-coated Sepharose beads (Amersham Pharmacia Biosciences). For the first-round selection, the amount of initial ssDNA pool was 10 nmol, dissolved in 1 ml of binding buffer, and the counterselection step was eliminated. To acquire aptamers with high affinity and specificity, the wash strength was enhanced gradually by extending wash time (from 1 to 10 min) and increasing the volume of wash buffer (from 0.5 to 5 ml) and the number of washes (from three to five). Additionally, 20% FBS and a 50- to 300-fold molar excess of genomic DNA were added to the incubation solution. After 20 rounds of selection, the selected ssDNA pool was PCR-amplified by using unmodified primers and cloned into *Escherichia coli* by using the TA cloning kit (Invitrogen). Cloned sequences were determined by the Genome Sequencing Services Laboratory at the University of Florida.

Flow-Cytometric Analysis. To monitor the enrichment of aptamer candidates after selection, the FITC-labeled ssDNA pool was incubated with 2 $\times$ 10^5 CCRF-CEM cells or Ramos cells in 200 μl of binding buffer containing 20% FBS on ice for 50 min. Cells were washed twice with 0.7 ml of binding buffer (with 0.1% NaN_3) and suspended in 0.4 ml of binding buffer (with 0.1% NaN_3). The fluorescence was determined with a FACScan cytometer (BD Immunocytometry Systems) by counting 30,000 events. The FITC-labeled unselected ssDNA library was used as a negative control.

The binding affinity of aptamers was determined by incubating CCRF-CEM cells (5 $\times$ 10^5) on ice for 50 min in the dark with varying concentrations of FITC-labeled aptamer in a 500-μl volume

of binding buffer containing 20% FBS. Cells were then washed twice with 0.7 ml of the binding buffer with 0.1% sodium azide, suspended in 0.4 ml of binding buffer with 0.1% sodium azide, and subjected to flow-cytometric analysis within 30 min. The FITC-labeled unselected ssDNA library was used as a negative control to determine nonspecific binding. All of the experiments for binding assay were repeated two to four times. The mean fluorescence intensity of target cells labeled by aptamers was used to calculate for specific binding by subtracting the mean fluorescence intensity of nonspecific binding from unselected library DNAs (18, 19). The equilibrium dissociation constants (K_d) of the aptamer–cell interaction were obtained by fitting the dependence of fluorescence intensity of specific binding on the concentration of the aptamers to the equation $Y = B \max X/(K_d + X)$, using SigmaPlot (Jandel, San Rafael, CA).

To test the feasibility of using aptamers for recognition of cancer cells in real biological samples, FITC-labeled aptamers were mixed with R-phycoerythrin- or peridinin chlorophyll protein-labeled antibodies of CD2, CD3, CD4, CD5, CD7, CD19, and CD45, respectively, and incubated with 2×10^5 cancer cells and/or 2×10^5 cells in human bone marrow aspirates. After washing as described above, fluorescence was determined with a FACScan cytometer (BD Immunocytometry Systems).

Confocal Imaging of Cell Bound with Aptamer. For confocal imaging, the selected ssDNA pools or aptamers were labeled with TAMRA. Cells were incubated with 50 pmol of TAMRA-labeled ssDNA in 100 μl of binding buffer containing 20% FBS on ice for 50 min. Other treatment steps were the same as described in *Flow-Cytometric Analysis*. Twenty microliters of cell suspension bound with TAMRA-labeled ssDNA was dropped on a thin glass slide placed above a ×60 objective on the confocal microscope and then covered with a coverslip. Imaging of the cells was performed on an Olympus FV500-IX81 confocal microscope. A 5-mW, 543-nm He-Ne laser was the excitation source for TAMRA throughout the experiments. The objective used for imaging was a PLAPO60XO3PH ×60 oil-immersion objective with a numerical aperture of 1.40 (Olympus).

Proteinase Treatment for Cells. CCRF-CEM cells (5×10^6) were washed with 2 ml of PBS and then incubated with 1 ml of 0.05% trypsin/0.53 mM EDTA in HBSS or 0.1 mg/ml proteinase K in PBS at 37°C for 2 and 10 min. FBS was then added to quench the proteinases. After washing with 2 ml of binding buffer, the treated cells were used for aptamer-binding assay as described in *Flow-Cytometric Analysis*.

We thank Ms. Kim Ahrens for help with cell culture and flow cytometry analyses, Ms. Regina Shaw and Dr. William Farmerie for help with DNA sequencing, Ms. Hui Lin for help with DNA synthesis, and Mr. Patrick Conlon for the schematic drawing. This work was supported by National Institutes of Health grants and a National Science Foundation Nanoscale Interdisciplinary Research Teams grant.

1. Luo, J., Isaacs, W. B., Trent, J. M. & Duggan, D. J. (2003) *Cancer Invest.* **21,** 937–949.
2. Espina, V., Geho, D., Mehta, A. I., Petricoin, E. F., III, Liotta, L. A. & Rosenblatt, K. P. (2005) *Cancer Invest.* **23,** 36–46.
3. Osborne, S. E. & Ellington, A. D. (1997) *Chem. Rev.* **97,** 349–370.
4. Nutiu, R. & Li, Y. (2005) *Angew. Chem. Int. Ed.* **44,** 1061–1065.
5. Wilson, D. S. & Szostak, J. W. (1999) *Annu. Rev. Biochem.* **68,** 611–647.
6. Breaker, R. R. (2004) *Nature* **432,** 838–845.
7. Ellington, A. D. & Szostak, J. W. (1990) *Nature* **346,** 818–822.
8. Tuerk, C. & Gold, L. (1990) *Science* **249,** 505–510.
9. Fang, X., Sen, A., Vicens, M. & Tan, W. (2003) *ChemBioChem* **4,** 829–834.
10. Guo, K., Wendel, H. P., Scheideler, L., Ziemer, G. & Scheule, A. M. (2005) *J. Cell. Mol. Med.* **9,** 731–736.
11. Yang, C. J., Jockusch, S., Vicens, M., Turro, N. & Tan, W. (2005) *Proc. Natl. Acad. Sci. USA* **102,** 17278–17283.
12. Liu, J. W. & Lu, Y. (2006) *Angew. Chem. Int. Ed.* **45,** 90–94.
13. Morris, K. N., Jensen, K. B., Julin, C. M., Weil, M. & Gold, L. (1998) *Proc. Natl. Acad. Sci. USA* **95,** 2902–2907.
14. Blank, M., Weinschenk, T., Priemer, M. & Schluesener, H. (2001) *J. Biol. Chem.* **276,** 16464–16468.
15. Daniels, D. A., Chen, H., Hicke, B. J., Swiderek, K. M. & Gold, L. (2003) *Proc. Natl. Acad. Sci. USA* **100,** 15416–15421.
16. Wang, C., Zhang, M., Yang, G., Zhang, D., Ding, H., Wang, H., Fan, M., Shen, B. & Shao, N. (2003) *J. Biotechnol.* **102,** 15–22.
17. Jayasena, S. D. (1999) *Clin. Chem.* **45,** 1628–1650.
18. Davis, K. A., Abrams, B., Lin, Y. & Jayasena, S. D. (1996) *Nucleic Acids Res.* **24,** 702–706.
19. Davis, K. A., Lin, Y., Abrams, B. & Jayasena, S. D. (1998) *Nucleic Acids Res.* **26,** 3915–3924.